THE JOURNAL OF BIOLOGICAL CHEMISTRY
Vol. 274, No. 19, Issue of May 7, pp. 13281–13291, 1999

Printed in U.S.A.

Glucose Generates Sub-plasma Membrane ATP Microdomains in Single Islet β-Cells

POTENTIAL ROLE FOR STRATEGICALLY LOCATED MITOCHONDRIA*

(Received for publication, June 18, 1998, and in revised form, February 10, 1999)

Helen J. Kennedy, Aristea E. Pouli‡, Edward K. Ainscow, Laurence S. Jouaville§, Rosario Rizzuto§, and Guy A. Rutter¶

From the Department of Biochemistry, School of Medical Sciences, University of Bristol, Bristol BS8 1TD, United Kingdom and the §Department of Biomedical Sciences and CNR Centre for Study of Biological Membranes, University of Padova, Via Trieste 75, 35121 Padua 17, Italy

Increases in the concentration of free ATP within the islet β-cell may couple elevations in blood glucose to insulin release by closing ATP-sensitive K^+ (K_{ATP}) channels and activating Ca^{2+} influx. Here, we use recombinant targeted luciferases and photon counting imaging to monitor changes in free [ATP] in subdomains of single living MIN6 and primary β-cells. Resting [ATP] in the cytosol ($[ATP]_c$), in the mitochondrial matrix ($[ATP]_m$), and beneath the plasma membrane ($[ATP]_{pm}$) were similar (~1 mM). Elevations in extracellular glucose concentration (3–30 mM) increased free [ATP] in each domain with distinct kinetics. Thus, sustained increases in $[ATP]_m$ and $[ATP]_{pm}$ were observed, but only a transient increase in $[ATP]_c$. However, detectable increases in $[ATP]_c$ and $[ATP]_{pm}$, but not $[ATP]_m$, required extracellular Ca^{2+}. Enhancement of glucose-induced Ca^{2+} influx with high $[K^+]$ had little effect on the apparent $[ATP]_c$ and $[ATP]_m$ increases but augmented the $[ATP]_{pm}$ increase. Underlying these changes, glucose increased the mitochondrial proton motive force, an effect mimicked by high $[K^+]$. These data support a model in which glucose increases $[ATP]_m$ both through enhanced substrate supply and by progressive Ca^{2+}-dependent activation of mitochondrial enzymes. This may then lead to a privileged elevation of $[ATP]_{pm}$, which may be essential for the sustained closure of K_{ATP} channels. Luciferase imaging would appear to be a useful new tool for dynamic *in vivo* imaging of free ATP concentration.

Increases in extracellular glucose concentration stimulate the exocytosis of insulin from islet β-cells. This is probably achieved by an increase in glycolysis and flux through the citrate cycle (1), leading to elevated intracellular levels of likely coupling factors (2), including ATP. Closure of ATP-sensitive K^+ channels (3–5) then leads to plasma membrane depolarization and the influx of Ca^{2+} through voltage gated Ca^{2+} channels.

Increases in the total intracellular concentration of ATP have been measured in isolated islets (6) and cell lines (7) exposed to increases in extracellular glucose concentration. However, the measured changes are generally small and difficult to interpret because of the large depot of intragranular ATP, and the presence of non-β-cells (8). Furthermore, such measurements give no indication of the concentration of unbound ATP. Unfortunately, measurements of free [ATP] in living cells, for example by ^{31}P NMR (9), cannot easily be extended to the islet micro-organ and do not provide sufficient sensitivity to detect changes at the cellular or subcellular level. This is an important question because differences in [ATP] at different intracellular sites have been predicted. In particular, locally high ATP consumption by the plasma membrane Na^+-K^+ and Ca^{2+}-ATPase, may mean that [ATP] is lower in this domain than in the bulk of the cell cytosol (1). Similarly, the electrogenic nature of the mitochondrial ATP/ADP translocase (10) is predicted to create differences in ATP/ADP ratio across the inner mitochondrial membrane (cytosolic high).

The role of changes in free Ca^{2+} ion concentration ($[Ca^{2+}]$) in regulating β-cell metabolism and ATP concentration is controversial. Increases in $[Ca^{2+}]$ following plasma membrane depolarization act both to stimulate ATP requiring processes (*i.e.* secretory granule movement and exocytosis) (11) and possibly to enhance mitochondrial oxidative metabolism (12, 13). Recent measurements of total ATP content of whole islets have suggested that the former may dominate and that Ca^{2+} influx may diminish glucose-induced increases in ATP/ADP ratio (14).

The use of firefly luciferase, targeted to discrete intracellular domains, should provide an extremely sensitive method of monitoring free [ATP] dynamically and at the subcellular level. In previous studies, we have shown that photon counting imaging of total luciferase activity in single cells provides a convenient means to measure changes in gene expression in single cells (15, 16). Luciferase has previously been employed to measure intracellular ATP concentration in single cardiac myocytes (17) and hepatocytes (18), but only after microinjection of the purified protein. In recent reports, Maechler *et al.* (19, 20) have shown that expression of recombinant luciferase provides a means of monitoring cytosolic ATP concentration in large populations (>10,000) of INS-1 β-cells. Unfortunately, such measurements fail to take account of the likely heterogeneity in the behavior of individual β-cells (21). Here, we use photon counting to image ATP concentrations dynamically and at the subcellular level in single living primary β-cells and derived MIN6 cells. We further extend this technique to allow the imaging of [ATP] in two cellular subdomains, the mitochondrial matrix and the subplasmallemal region, by the molecular targeting of luciferase. We demonstrate that exposure to elevated glucose concentrations causes increases in [ATP] in each of the compartments analyzed, coincident with an increase in mitochon-

* We thank for financial support the Wellcome Trust, the Medical Research Council (United Kingdom), the Royal Society, the British Diabetic Association, the Christine Wheeler Bequest, Italian "Telethon" (project no. 850), the "Biomed" program of the European Union, and the Italian University Ministry (to R. R.). The costs of publication of this article were defrayed in part by the payment of page charges. This article must therefore be hereby marked "*advertisement*" in accordance with 18 U.S.C. Section 1734 solely to indicate this fact.

‡ A Bristol University Research Scholar.

¶ To whom correspondence should be addressed. Tel.: 44-117-928-9724; Fax: 44-117-928-8274; E-mail: g.a.rutter@bris.ac.uk.

drial membrane potential. Comparison of the kinetics of [ATP] changes, and dependence on increases in mitochondrial free $[Ca^{2+}]$ ($[Ca^{2+}]_m$),[1] also suggests that activation of strategically located mitochondria may preferentially enhance [ATP] immediately beneath the plasma membrane.

MATERIALS AND METHODS

Plasmid Construction—Cytosolic (untargeted) firefly luciferase in plasmid pGL3 basic (Promega) was placed under cytomegalovirus immediate gene control by subcloning the cytomegalovirus promoter element from plasmid pcDNA3 (Invitrogen) as an 876-nucleotide *Bgl*II-*Hin*dIII fragment into the upstream multiple cloning site of pGL3, generating plasmid cLuc. Plasma-membrane targeted luciferase was prepared by polymerase chain reaction amplification of the 617-nucleotide translated region (minus stop codon) of synaptosome-associated protein of 25 kDa cDNA, with primers 5′ T.TTT.GAC.GAG.ACC.ATG-.GCC.GAG.GAC.GCA and 5′TT.TTC.CAT.GGT.ACC.ACT.TCC.CAG-.CAT.CTT (*Nco*I sites underlined) and the 629-nucleotide polymerase chain reaction fragment digested and subcloned into the plasmid pGL3-control (Promega) under SV40 immediate early gene promoter control, generating plasmid pmLuc. Correct orientation of the insert was verified by restriction mapping with *Sma*I and *Sal*I, and confirmed by automated DNA sequencing. To allow higher levels of expression of this construct under cytomegalovirus promoter control, the *Hin*dIII-*Bam*HI fragment of pmLuc was subcloned into plasmid pcDNA3; essentially identical data were obtained with either plasmid. For the preparation of mLuc, DNA sequences encoding a mitochondrial presequence and the hemagglutinin HA1 tag were added to the luciferase cDNA as follows. A fragment of wild-type luciferase cDNA was first amplified from plasmid pGL2 (Promega) using the following primer: 5′AAAG.CTT.AAT.GGA.AGA.CGC.CAA.AAA.CAT.AAA.GAA.A (corresponding to the sequence encoding amino acids 1–9 of luciferase; *Hin*dIII site underlined) and GAA.GAT.GTT.GGG.GTG.TTG.TAA.CAA.T (downstream of the endogenous *Cla*I site of the luciferase cDNA and encoding amino acids 456–465). The polymerase chain reaction product was digested with the enzymes *Hin*dIII and *Cla*I and fused in frame to the *Cla*I/*Hin*dIII fragment encoding the HA1 tag (22). A *Cla*I fragment was thus generated that, in an appropriately prepared pBSK+ plasmid, could be fused in frame with the *Eco*RI/*Hin*dIII fragment encoding the amino-terminal 33 amino acids of cytochrome oxidase subunit 8 (COX8) (25 amino acids of the cleavable presequence plus 8 amino acids of the mature polypeptide) (23) and the *Cla*I/*Sal*I fragment encoding the carboxyl-terminal portion of luciferase (amino acids 457–556). The whole final construct (shown schematically in Fig. 1) was excised via *Pst*I/*Sal*I digestion and cloned into the expression vectors VR1012 (Vical Research Inc., San Diego, CA) under modified cytomegalovirus promoter control.

Cell Culture, Microinjection, and Imaging—Primary rat islet β-cells were isolated by collagenase (PanPlus, Serva) digestion and purified on a discontinuous bovine serum albumin gradient (16). Cells were dissociated with trypsin before 24 h culture on Cell-Tak™-treated glass coverslips. Plasmids (0.2–0.4 mg·ml^{-1} in 10 mM Tris, 0.2 mM EDTA) were microinjected using glass borosilicate capillaries and an Eppendorf 5171 transjector/micromanipulator, as described (16, 24). MIN6 cells were cultured on poly-L-lysine-treated coverslips (25). Injected primary β-cells cells were cultured 16–24 h in an atmosphere 5% CO_2, and at 3 mM glucose. For all experiments in which the effects of elevated glucose or K^+ concentrations were tested, MIN6 cells were cultured at 3 mM glucose for 24 h before imaging. Such cells responded robustly to elevated glucose concentrations with enhanced insulin secretion (4–10-fold above basal levels) (26). Cells were imaged in modified Krebs-Ringer bicarbonate medium (0.2 ml) comprising 125 mM NaCl; 3.5 mM KCl; 1.5 mM $CaCl_2$; 0.5 mM $MgSO_4$; 0.5 mM KH_2PO_4; 2.5 mM $NaHCO_3$, 10 mM Hepes-Na^+, pH 7.4, containing the indicated glucose concentration and equilibrated with 95:5 O_2:CO_2. Cells were maintained on the temperature-controlled (37 °C) stage of an Olympus IX-70 microscope (UPlanApo × 10, 0.4 numerical aperture air objective), located in a sealed dark housing. Medium was rapidly (<2 s) changed by the addition of an equal volume through a remotely located syringe. For calibration of signals, cells were lysed in "intracellular medium" comprising 20 mM Hepes, 140 mM KCl, 5 mM NaCl, 10.2 mM EGTA, 6.67 mM $CaCl_2$, 1 mM luciferin, 20 μg·ml^{-1} digitonin plus additions of ATP, $MgSO_4$, and CoA as indicated. Data were captured with an intensified charge-coupled device camera comprising a low-noise S-20 multi-alkali photocathode and three in-series microchannel plates (Photek ICCD216; Photek Ltd., St. Leonards-on-Sea, East Sussex, United Kingdom), maintained at 4 °C. Single photon events were captured at 25-ms intervals by time-resolved imaging, which allowed the spatial and temporal coordinates of each photon event to be held in matrix format. In this way, luminescence changes of any individual cell or group of cells could be analyzed for the entire time course of an individual experiment. When required, images corresponding to the selected area of interest within the image field were generated retrospectively over the desired integration period. Aequorin imaging was performed in cells expressing mitochondrially targeted aequorin (27) as described previously (24).

Measurements of Tetramethylrhodamine Ethyl Ester (TMREE) Fluorescence—Cells were maintained at 37 °C for 2 h in serum-free Dulbecco's modified Eagle's medium containing 3 mM glucose, and then loaded with TMREE (10 nM) for 60 min. Confocal imaging was performed in KREBS, initially containing 3 mM glucose, using a Leica TCS-NT inverted confocal microscope, fitted with a × 40 oil immersion objective, with illumination at 568 nm from a krypton/argon laser. Fluorescence from groups of 4–7 single cells was analyzed off-line; this compensated for the considerable movement of individual mitochondria in and out of the confocal plane.

Immunocytochemistry—Cells were fixed and permeabilized 24 h after microinjection using 4% (v/v) paraformaldehyde plus 0.2% Triton X-100. Primary polyclonal rabbit anti-luciferase antibody (Promega) was revealed with tetra-methyl-rhodamine-conjugated anti-rabbit immunoglobulin G (Sigma). Confocal images were obtained using a Leica TCS 4D/DM IRBE laser scanning confocal microscope equipped with a krypton/argon laser (568 nm excitation line) and analyzed off-line using a Silicon Graphics workstation.

Kinetic Analysis of Luciferase in Vitro—MIN6 cells were transiently transfected with the lipoamine Tfx-50™ (Promega) as per the manufacturer's instructions. Cells were extracted into buffer comprising 20 mM Hepes, 0.1% Triton X-100 (pH 7.2) and assayed in intracellular medium (see above) using an LB-9501 luminometer (EG & Berthold, Bad Wildbad, Germany).

Statistical Analysis and Other Methods—Data are presented as means ± S.E. for the number of observations given. For K_m measurement of the different luciferases, statistical significance was determined by Fischer test for the improvement in fitting individual K_m values compared with fitting a common value (28). ATP content of MIN6 cell populations was determined in extracts using firefly lantern extracts (29). Intracellular pH was measured by monitoring fluorescence changes at the single cell level using 2′7′-bis(carboxyethyl) 5(6)carboxyfluorescein as an intracellular pH indicator. Briefly, cells grown on glass coverslips and preloaded with 2′7′-bis(carboxyethyl) 5(6)carboxyfluorescein for 20 min were perifused continuously with Krebs-Ringer bicarbonate medium at a flow rate of 2 ml min^{-1} on the stage of a Nikon Diaphot microscope equipped with a × 40 oil immersion objective. The ratio of the emitted light at two excitation wave lengths (440/490 nm) was used to monitor intracellular pH, using commercially available software (Cairn Instruments, Faversham, Kent, United Kingdom) for data acquisition.

RESULTS

Expression and Calibration of Targeted Firefly Luciferases—Luminescence imaging of firefly luciferase provides adequate resolution at the single cell level but is not readily amenable to confocal or deconvolution methods necessary to achieve subcellular resolution (24). We therefore used the molecular approach of targeting luciferase to distinct subcellular domains by fusion with specific peptide sequences. Fig. 1 shows the constructs used in this study. Mitochondrially targeted luciferase (mLuc) was based on wild-type *Photinus pyralis* firefly luciferase (M_r 65 kDa), extended at the amino terminus via the 26-amino acid amino-terminal signal peptide of cytochrome *c* oxidase subunit VIII (23). This presequence is cleaved soon after mitochondrial import of the parental protein (30). pmLuc was generated by fusion with synaptosome-associated protein of 25 kDa, a neuoronal v-SNARE (11) targeted to the plasma membrane and neurite extensions after palmitoylation at two amino-ter-

[1] The abbreviations used are: $[Ca^{2+}]_m$, $[Ca^{2+}]_c$, and $[Ca^{2+}]_{pm}$, free Ca^{2+} concentration in the mitochondrial matrix, cytosol, and plasma membrane regions, respectively; cLuc, cytosolic firefly luciferase; mLuc, mitochondrial matrix firefly luciferase; pmLuc, plasma membrane firefly luciferase; ΔΨ, mitochondrial membrane potential, TMREE, tetramethylrhodamine ethyl ester.

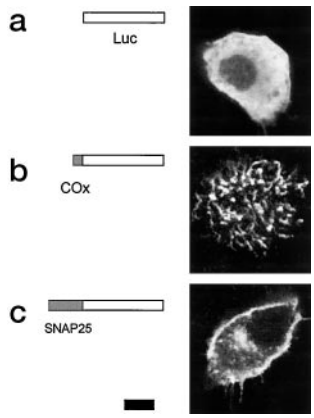

FIG. 1. **Targeting strategies for firefly luciferase.** *a,* cLuc; *b,* mLuc; *c,* pmLuc. Cytosolic luciferase (lacking the carboxyl-terminal Ser-Lys-Leu peroxisomal targeting motif (38) and engineered for optimal codon usage in mammalian cells) provided the basis for cLuc and pmLuc, and wild-type luciferase provided the basis for mLuc. MIN6 cells were microinjected and cultured 24 h before fixation, permeabilization, and immunocytochemical analysis (see under "Materials and Methods"). Individual optical slices (0.5 μm) are shown. *Black bar* represents 100 nucleotides.

minal cysteine residues (31). These constructs targeted luciferase to the mitochondrial matrix and the plasma membrane respectively (Fig. 1), as predicted from the behavior of aequorin and green fluorescent protein targeted by identical strategies (32, 33). Limited localization (< 10% of total) to a vesicular, intracellular compartment was also observed after expression of pmLuc and may represent association with secretory vesicles (34).

The sensitivity of recombinant expressed luciferase to [ATP] was first determined in cell extracts. These assays were performed in the presence of likely intracellular concentrations of CoA (0.01 mM) (35), a known regulator of enzyme activity (36). The presence of CoA greatly reduces the complex "flash" kinetics of the enzyme, believed to result either from the formation of the luciferyl·AMP intermediate, or the accumulation of the reaction product, oxyluciferin (37), probably by enhancing the breakdown of the less stable enzyme·luciferyl·CoA intermediate (36, 38). Calibration of the responses of each expressed and extracted luciferase to [ATP] indicated a similar K_m for [ATP] of each construct, close to 1 mM (Fig. 2).

We next demonstrated that luminescence from the expressed recombinant chimeras could be imaged in single living cells over the likely time frame of changes in intracellular [ATP]. Photon production was imaged in single luciferase-expressing MIN6 cells using an intensified and cooled charge-coupled device camera (15, 39) attached to an inverted optics microscope equipped with a × 10 objective lens. In the presence of 1 mM luciferin, this technique allowed 2–5-s resolution in MIN6 cells, in which high levels of luciferase expression could be achieved, and 5-s resolution in primary β-cells (see below, Fig. 8). As observed previously (40) this concentration of luciferin was close to saturating for photon production by single cells, with little further increase in luminescence observed in the presence of 2 mM luciferin or above (data not shown). Ouabain (100 μM) caused a small increase in luminescence from cells expressing cLuc (5 ± 1%, n = 16 cells) but a more substantial increase in luminescence from cells expressing pmLuc (14 ± 1.5%, n = 15 cells) and mLuc (11.5 ± 1.5%, n = 16), as expected by the relief of ATP consumption by the plasma membrane Na^+/K^+-ATPase. It should be noted that these and smaller changes could readily be detected. Indeed, changes in luminescence in populations of 8–12 cells of as little as 3% were found to be statistically significant when integrated over a 40-s interval (results not shown).

To determine the value of [ATP] in each subcompartment, we monitored the luminescence of single cells before and after permeabilization in the presence of ATP (Fig. 2). Single MIN6 cells were permeabilized with digitonin at the likely subdomain pH (7.2 for the cytosol and sub-plasma membrane region, or pH 7.8 for the mitochondrial matrix), intracellular free CoA (0.01 mM) (35) and Mg^{2+} (0.5 mM) (41, 42). Permeabilization caused a time-dependent decrease in luminescence from each construct, presumably reflecting loss of ATP from the cell cytosol or conversion of intramitochondrial ATP to ADP (for mLuc). Re-addition of ATP caused the re-appearance of luminescence after an initial small burst, as observed in extracts (Fig. 2). Comparison of the steady-state luminescence level before and after permeabilization with the obtained standard curves indicated resting [ATP] values in the low mM range in each compartment (Fig. 2).

Role of Factors Other Than Intracellular [ATP] in Photon Production by Recombinant Luciferases in MIN6 Cells—To confirm that any stimulus-induced luminescence change was due, principally, to changes in intracellular [ATP] and was unlikely to be the result of changes in the concentration of other luciferase substrates or effectors, we monitored the effects of changes in these parameters on firefly luciferase activity *in vitro* and in living cells. Because luciferase activity was increased *in vitro* by increases in pH (activity at 1 mM ATP: 1.0, 1.2, and 1.4 arbitrary units at pH 6.8, 7.2, and 7.6, respectively), we first investigated whether pH changes may contribute to any observed luminescence change in response to cell stimulation. Transient intracellular alkalinization of cells with 10 mM NH_4Cl increased the luminescence output from cells expressing each construct by 15–20%, whereas acidification with 10 mM Na^+ acetate caused a decrease in light output by about the same amount. Under the conditions used in these studies, exposure of MIN6 cells to 30 mM glucose caused little or no change in intracellular pH (26). However, 70 mM K^+ caused a small (3–5%) decrease in 2′7′-bis(carboxyethyl) 5(6)carboxyfluorescein fluorescence ratio, which could be mimicked by treatment with 4 mM Na^+-acetate (data not shown), likely to correspond to a pH decrease of < 0.05 pH units (43). We next tested the effects of increasing CoA concentration on extracted luciferase. In islets, Liang and Matschinsky (35) have reported that increasing extracellular glucose from 2.5 to 25 mM raised islet CoA content by about 6% during a 30-min perfusion, from 6.8 pmol/μg DNA (equivalent to 6.8 μmol/liter, assuming 10 ngDNA·islet^{-1}, and a cell volume of 2 pl) to 7.2 pmol/μg DNA. In our hands, a 500% increase in [CoA], from 10 to 50 μM, was required to increase luciferase luminescence in cell extracts by 28%. It should be noted that an increase in intracellular concentration of O_2, another key luciferase substrate, is unlikely in response to elevated extracellular glucose concentrations, because these usually provoke increases in O_2 consumption (44) and an increased intracellular NAD(P)H/$NAD(P)^+$ ratio (see below). Finally, no changes in the luminescence were apparent in cells transfected with the non-ATP-utilizing luciferase from the sea pansy, *Renilla reniformis* (16) (data not shown).

Control of Mitochondrial [ATP] by Glucose and Intracellular Ca^{2+}—As a functional assay of the correct targeting of mitochondrial luciferase in living cells, we determined whether $[ATP]_c$ and $[ATP]_m$ could be altered independently in the presence of atractyloside, a potent inhibitor of the mitochondrial adenine nucleotide translocase (10). As shown in Fig. 3, exposure to atractyloside caused a time-dependent decrease in luminescence from cells microinjected with cytosolic luciferase (Fig. 3). By contrast, in cells microinjected with cDNA encoding mitochondrial luciferase, an anti-parallel increase in the lumi-

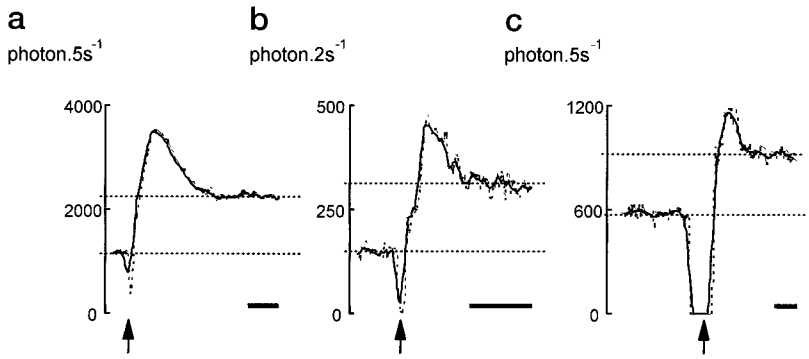

FIG. 2. **Dependence of luciferase activity on [ATP] *in vivo.*** *a–c,* photon production by 6–30 single living MIN6 cells was measured by photon counting digital imaging (see under "Materials and Methods") in the Krebs-Ringer bicarbonate medium containing 1 mM luciferin. Cells were imaged 24 h after microinjection with cLuc (*a*), mLuc (*b*), or pmLuc (*c*). After establishment of a steady state of photon production, the camera was switched off (resulting in the observed decrease in photon detection rate), and cells were permeabilized by the replacement of the medium with intracellular medium containing 20 $\mu g \cdot ml^{-1}$ digitonin plus 10 mM ATP and 9–10.5 mM $MgCl_2$. *Broken traces* correspond to data integration over 2 s, and *solid lines* correspond to a rolling average of between 5 (*a* and *b*) and 15 (*c*) individual points. Permeabilization in the absence of added ATP caused a time-dependent decrease in single cell luminescence to <30 photon·s^{-1} over the whole field, close to the observed dark count (in the absence of cells) for this camera. These data were essentially unaffected by the addition of ADP over the likely range of free intracellular concentration, 0.1–1.0 mM. At all ATP concentrations tested, luminescence was absolutely dependent upon the presence of Mg^{2+} ions consistent with MgATP as the true substrate of the luciferase reaction. At the free [Mg^{2+}] used in these studies (0.5 mM), approximately 90% of ATP is in the $MgATP^{2-}$ form, such that these K_m values closely represent the K_m for $MgATP^{2-}$. *Horizontal broken lines* indicate the pre- and post-ATP addition steady state levels from which the intracellular ATP concentrations were obtained. *Bars* indicate 120 s. Kinetic analyses were performed using soluble extracts of cells transfected with cLuc (*a*), mLuc (*b*), or pmLuc (*c*). Light output was measured using a photon counting luminometer in intracellular medium (see under "Materials and Methods") supplemented with 0.01 mM CoA at pH 7.2 (cLuc and pmLuc) or pH 7.8 (mLuc). $MgCl_2$ was added in the range 1.5–10 mM to provide a constant free Mg^{2+} concentration of 0.5 mM, calculated using METLIG software (85). Light output was integrated over 30 s. Calculated K_m values (mM) for ATP were obtained by nonlinear regression analysis (FigP, Cambridge Biosoft, Cambridge United Kingdom) assuming Michaelis-Menten kinetics, using ATP concentrations in the range 0.1–10 mM. Combining data from three entirely separate luciferase preparations gave K_m values (in mM) of: cLuc, 1.18 ± 0.45; mLuc, 1.67 ± 0.61; and pmLuc, 0.65 ± 0.13. No statistically significant difference (see under "Materials and Methods") was revealed between the K_m values for luciferase expressed in different compartments. Assuming these constants, the above experiment gave values for $[ATP]_c$, $[ATP]_m$, and $[ATP]_{pm}$ of 1.0, 1.2, and 0.9 mM, respectively.

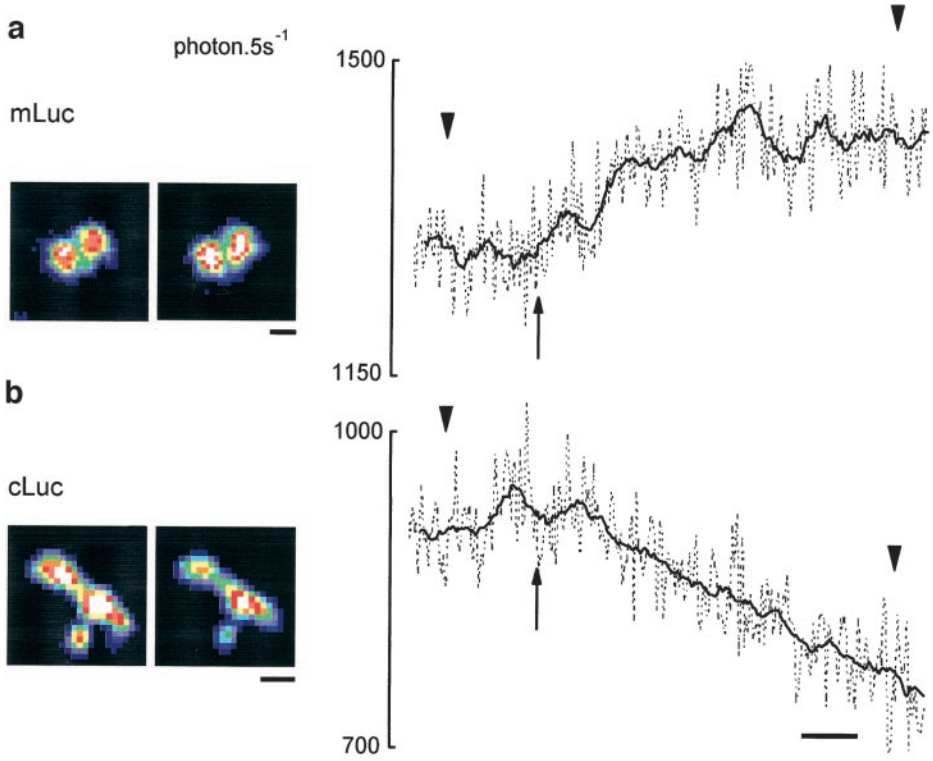

FIG. 3. **Effect of atractyloside on luminescence from populations of single MIN6 cells expressing mLuc (*a*) or cLuc (*b*).** Populations of cells expressing luciferase in the mitochondrial matrix (*a*) (15 cells) or cytosol (*b*) (18 cells) were imaged in the presence of 3 mM glucose. Atractyloside (50 μM) was added at the *upward arrow*. Panels show the luminescence of single cells during a 20-s integration beginning at the position of the *downward arrowheads*. *Bars* beneath the panels correspond to 15 μm, and the *time bars* correspond to 120 s. Pseudocoloring is as follows: *black,* 0; *blue,* 1–5; *green,* 6–7; *yellow,* 8–9; *red,* 10–12; and *white,* ≥13 photon·s^{-1}·$pixel^{-1}$.

nescence of mitochondrial luciferase was apparent.

Exposure to 30 mM glucose of MIN6 cells expressing mLuc provoked a rapid, stable (for at least 10 min) increase in luminescence (Fig. 4, *a* and *b*). Blockade of Ca^{2+} influx slowed the apparent glucose-induced $[ATP]_m$ increase but had little or no effect on the final extent of the $[ATP]_m$ change (Fig. 4*b*; Table I). Furthermore, the effect of glucose could be mimicked, in part, by an increase in intracellular [Ca^{2+}], provoked by exposure to high [K^+] (Fig. 5, *a* and *b*). Unlike the stable luminescence increase observed in response to elevated glucose, this K^+-induced $[ATP]_m$ increase was transient (Fig. 5*a*; Table I). Simultaneous addition of glucose and high [K^+] caused a substantial decreased the half-time for the glucose-induced $[ATP]_m$ increase and a small increase in the maximum extent of the luminescence change, compared with glucose alone (Table I). Confirming that changes in $[Ca^{2+}]_c$ or $[Ca^{2+}]_m$ were central to

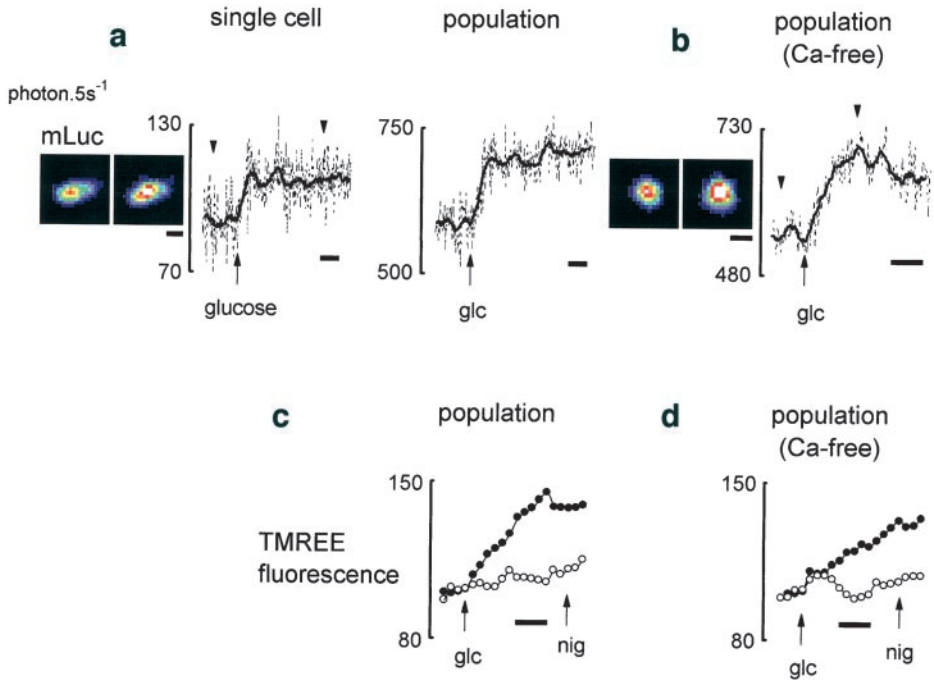

FIG. 4. **Control of $[ATP]_m$ and $\Delta\Psi$ by glucose.** In *a,* luminescence was measured from a single cell (*left*) or a population of 51 single cells (*right*) expressing mLuc, whereas TMREE fluorescence (*c* and *d*) was monitored as described under "Materials and Methods." Dashed traces in *c* and *d* correspond to changes observed in the absence of additions. Where indicated, [glucose] was increased to 30 mM (*glc*), whereas nigericin (2 μM) (*nig*) was added as indicated to TMREE-loaded cells. Data shown in *traces b* and *d* were from populations of 16 and 13 single cells, respectively, maintained in the absence of extracellular Ca^{2+} (medium supplemented with 1 mM EGTA). Images of single cells (*inserts* in *a* and *b*) correspond to 30-s integrations of luminescence at the *downward arrowheads* shown. Scales and pseudocoloring are as in Fig. 3. *Dashed lines* in *c* and *d* show fluorescence changes observed in control, unstimulated cells.

TABLE I

Mean changes in [ATP]-dependent luminescence in the cytosol, mitochondrial matrix, and sub-plasma membrane region of single β- and MIN6 cells

Measurements of luciferase luminescence were performed as described in the legend to Figs. 2–4. Percentage increases were calculated at the peak luminescence change. Half-time values ($t_{1/2}$) for increases (+) to peak and decrease from the peak (−) were calculated by direct examination of rolling average data (*e.g.* see Fig. 3). The data shown correspond to means ± S.E. for the number of single cells and separate cultures given in parentheses. N.A., not applicable. Changes in luminescence represent increases, except for those marked (↓).

Cell type, construct, and condition	30 mM glucose			70 mM K^+			Glucose + K^+		
	Increase	$t_{1/2}$ (+)	$t_{1/2}$ (−)	Change	$t_{1/2}$ (+)	$t_{1/2}$ (−)	Increase	$t_{1/2}$ (+)	$t_{1/2}$ (−)
	%	*s*		%	*s*		%	*s*	
MIN6 cells									
mLuc control	15.7 ± 1.7	54.7 ± 10.7 (53; 3)[a]	N.A.	25.0 ± 1.15	24.3 ± 1.2 (57; 3)	230	21.1 ± 1.7	20.5 ± 1.5 (33; 2)	N.A.
+EGTA	23.5 ± 0.5	83.5 ± 3.5 (17; 2)	N.A.	15.0 ± 6.0 (↓) (40; 2)	N.A.	>200			
cLuc	15.7 ± 4.3	35.3 ± 2.4 (114; 3)	312	25.5 ± 10.4	15.0 ± 1.0 (47; 3)	86	10.1 ± 2.1	11.0 ± 1.0 (128; 2)	N.A.
+EGTA	0.0			15.0 ± 0.5 (↓) (28; 2)	N.A.	80			
pmLuc	13.4 ± 1.8	20.0 ± 1.2 (30; 3)	N.A.	29.8 ± 5.4	11 ± 0.6 (56; 4)	120	45.0 ± 10	10.3 ± 0.7 (20; 1)	N.A.
+EGTA	0.0			31.1 ± 6.4 (↓) (19; 2)	N.A.	>200			
Primary β-cells									
cLuc	10.4 ± 3.5	125 (5; 1)	N.A.	29.5 ± 2.5	43.0 ± 6.4 (35; 5)	150	47.5 ± 7.5	56.3 ± 3.8 (21; 2)	192

[a] First number in parentheses indicates single cells; second number indicates cultures.

the effects of K^+, addition of K^+ in the absence of external Ca^{2+} resulted in a marked decrease in $[ATP]_m$ (Fig. 5b, Table I).

To determine directly whether increases in intracellular $[Ca^{2+}]$ activated mitochondrial oxidation, and the contribution of this activation to the effect of glucose on $[ATP]_m$, we monitored on-line the mitochondrial membrane potential, $\Delta\psi$, after loading the cells with a dye, TMREE (Figs. 4, *c* and *d,* and 5, *c* and *d*), which rapidly equilibrates across the inner mitochondrial membrane according to $\Delta\Psi$ (45). Both elevated glucose and K^+ concentrations provoked time-dependent increases in mitochondrial fluorescence of cells loaded with TMREE. Thus, K^+ stimulation provoked a rapid, 33 ± 3% increase (n = 31 cells, 6 separate experiments) in $\Delta\psi$, that peaked after ~90 s (Fig. 5). By contrast, stimulation by glucose alone gave a slower, but more substantial, increase in fluorescence equal to 39 ± 6% (n = 16 cells, three separate experiments) after 6 min (Fig. 4). This glucose-induced increase in $\Delta\Psi$ thus occurred more slowly than $[ATP]_m$ (Fig. 4, *c versus a*). Similar to the effect on $[ATP]_m$, simultaneous addition of high $[K^+]$ with glucose provoked a peak response similar to that observed with K^+ alone, but then led to a time-dependent decrease in $\Delta\Psi$, which returned to prestimulatory values at extended time periods (> 300 s).

Changes in pH gradient across the mitochondrial inner membrane were assayed as the increase in fluorescence upon addition of nigericin, which allows exchange of K^+ for H^+ across the inner mitochondrial membrane (46). When added to naïve cells, nigericin caused an increase in TMREE fluorescence of 10 ± 2% (n = 7 cells, two separate experiments). Stimulation by glucose and K^+ appeared to diminish the size of the fluorescence change caused by the subsequent addition of nigericin to about half that observed in naïve cells. However, the relative sizes of the fluorescence changes suggest that stimulation of $\Delta\psi$ by K^+ and glucose outweigh any change in pH gradient, so that both stimuli caused a net increase in mitochondrial proton motive force (Figs. 4 and 5).

In the absence of extracellular Ca^{2+}, addition of K^+ caused a

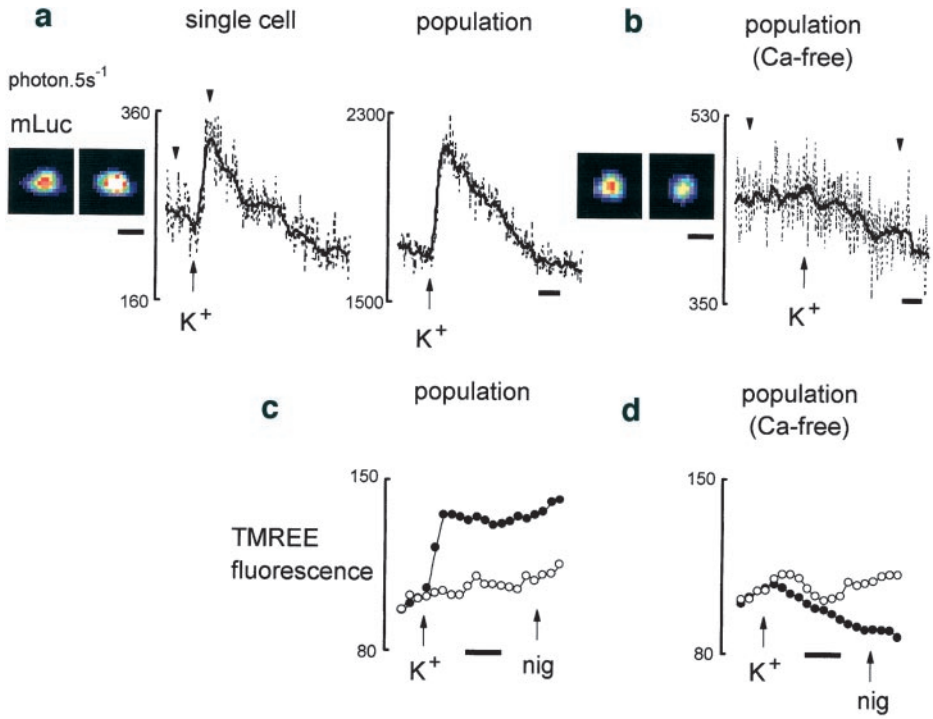

FIG. 5. **Control of $[ATP]_m$ by external K^+.** Measurements were performed essentially as described in Fig. 4, but with additions of 70 mM KCl (K^+) in place of additional glucose. Cell populations comprised 25 (*a*), 15 (*b*), 21 (*c*), or 15 (*d*) single cells.

decrease in TMREE fluorescence (Fig. 5*d*) that mirrored the decrease in $[ATP]_m$ provoked by K^+ in the absence of external Ca^{2+} (Fig. 5*b*). By contrast, stimulation with 30 mM glucose in Ca^{2+}-free medium gave an increase in fluorescence, of 30 ± 3% (n = 13 cells, three separate experiments) after 6 min, but the response was smaller and slower than that in the presence of external Ca^{2+} (Fig. 4*d*). This pattern of dependence on extracellular Ca^{2+} ions closely resembled that of $[ATP]_m$ (see above, Figs. 4 and 5). Together, these data indicate that the effect of glucose on $[ATP]_m$ may be mediated both by an increase in substrate supply and through the activation by Ca^{2+} of mitochondrial dehydrogenases and the respiratory chain.

In order to explore whether increases in intramitochondrial free $[Ca^{2+}]$ could be directly responsible for the measured elevations in intracellular free [ATP] in response to exposure to high K^+, we used the Ca^{2+}-sensitive photoprotein, recombinant aequorin, targeted to the mitochondrial matrix (24, 27, 47, 48). Challenge of cells with K^+ provoked a transient increase in mitochondrial $[Ca^{2+}]$, as indicated by a rapid burst in aequorin-derived luminescence (data not shown), which peaked 6 s after stimulation with K^+. Whether K^+ depolarization led to any further, sustained, increase in $[Ca^{2+}]_m$ could not be resolved conclusively with this approach, due to the limited sensitivity of aequorin in single cells (24). However, studies on MIN6 populations expressing mitochondrial aequorin (49) suggest that this may be the case.

Control of $[ATP]_c$ and $[ATP]_{pm}$ by Glucose and Ca^{2+} Ions—Exposure to elevated glucose concentrations (30 mM) caused a marked increase in both $[ATP]_c$ and $[ATP]_{pm}$ (Fig. 6, Table I). However, the kinetics of the subsequent changes were distinct in these two cytosolic compartments (Fig. 6; Table I). In particular, under conditions in which transient increases in $[ATP]_c$ were elicited by the elevation of glucose (Fig., 6), $[ATP]_{pm}$ was increased stably (Fig. 6*d*; Table I). In further contrast to the $[ATP]_m$ changes, removal of extracellular Ca^{2+} completely blocked detectable glucose-induced increases in both compartments (Fig. 6, *b* and *e*; Table I). Similarly, K^+-addition provoked an increase in $[ATP]_c$, which recovered more quickly than $[ATP]_m$ (compare Figs. 7 and 5 and see Table I). Depolarization of cells with high external $[K^+]$ also caused an increase in $[ATP]_{pm}$ in the sub-plasma membrane domain, which was closely similar in magnitude to the change in $[ATP]_c$, but of slightly longer duration (Fig. 7; Table I). Simultaneous addition of K^+ with glucose had no significant effect on the maximum extent of the glucose-induced increase in $[ATP]_c$ but instead slowed its relaxation to prestimulatory values (Table I). By contrast, co-addition of K^+ with glucose enhanced the initial increase in $[ATP]_{pm}$ but prompted a more rapid return to basal levels. K^+ addition at 3 mM glucose and in the absence of extracellular Ca^{2+} caused a marked decrease in both $[ATP]_c$ and $[ATP]_{pm}$ (Table I).

These clear changes in $[ATP]_c$ and $[ATP]_{pm}$ were not associated with any statistically significant change in total cellular ATP content after exposure to 70 mM K^+. Thus, the ATP content of unstimulated MIN6 cells was 1641 ± 415 pmol·100,000 cells^{-1}, compared with 1514 ± 372, 60 s after exposure to 70 mM K^+ (p = 0.08 with respect to unstimulated cells by paired Student's t test), and 1644 ± 371 pmol·100,000 cells^{-1} 120 s after K^+ stimulation (p = 0.49; n = 9 separate experiments, each comprising two MIN6 cultures).

Response of Primary Islet β-cells to Increases in Extracellular Glucose Concentration and Ca^{2+} Influx—We next determined whether the above observations, performed on a derived β-cell line, could be extended to primary living β-cells from adult animals. In primary, as opposed to clonal cells, it has been suggested that responses to increasing glucose concentration occur on an "all-or-nothing" basis, with increasing recruitment of individual cells with elevated [glucose] (50). Fig. 8 shows the changes in luminescence of β-cells, microinjected with plasmid cLuc and exposed 24 h later to elevated glucose concentrations or high (70 mM) K^+. Typical increases of the luminescence of single cells are represented in the pseudocolor images presented in Fig. 8.

As in MIN6 cells, increasing the concentration of glucose in the medium from 3 to 30 mM caused a time-dependent increase in luminescence, but here the increase was smaller

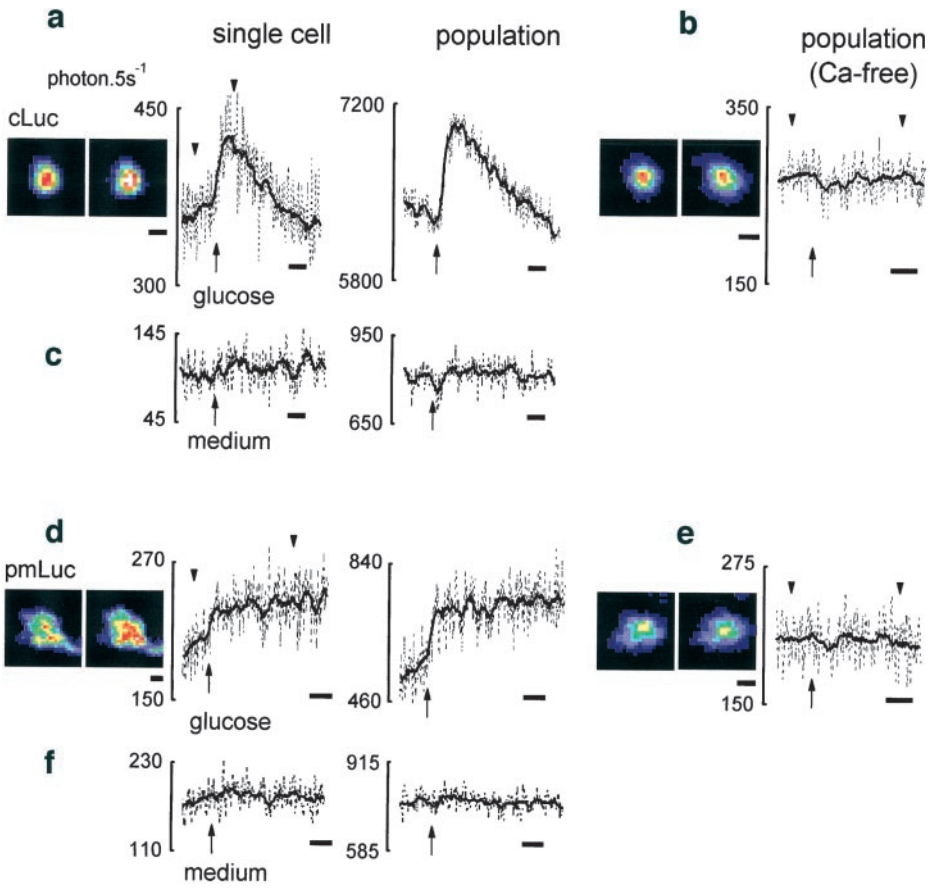

FIG. 6. **Control of $[ATP]_c$ and $[ATP]_{pm}$ by glucose.** Measurements of luminescence were performed as described in Fig. 4, using cells expressing cLuc (*a–c*) or pmLuc (*d–f*) as shown. *c* and *f* show the effects of control additions of medium (without 30 glucose). Pseudocolors and *scale bar* are as in Fig. 3. Experiments involved populations of 51 (*a*), 18 (*b*), 11 (*c*), and 8 (*d*) cells.

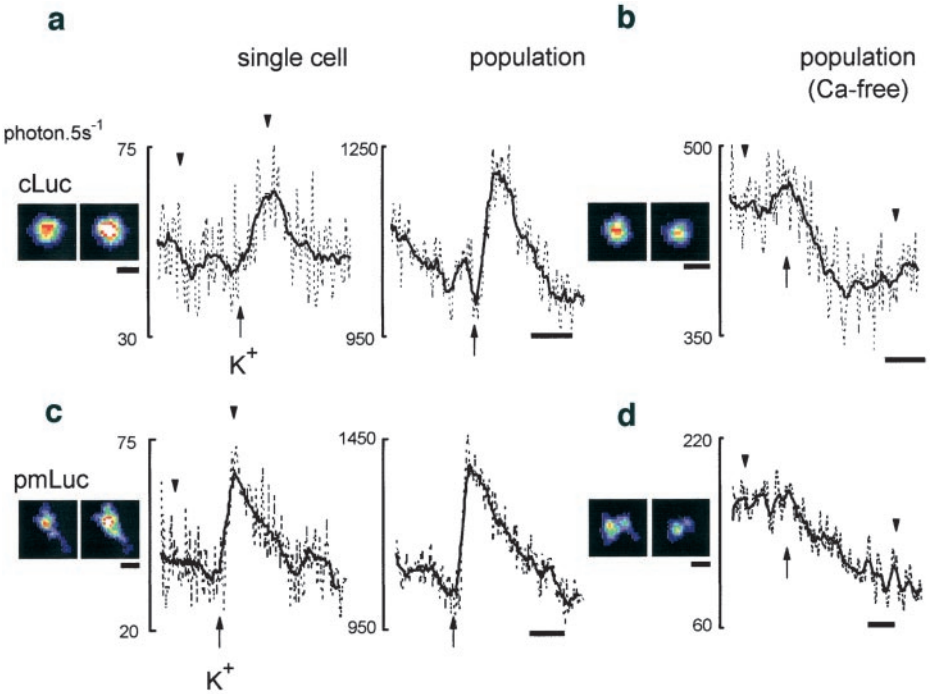

FIG. 7. **Control of $[ATP]_c$ and $[ATP]_{pm}$ by K^+.** Measurements of luminescence were performed as described in Fig. 5, using cells expressing cLuc (*a* and *b*) or pmLuc (*c* and *d*) as shown. Pseudocolors and *scale bar* are as in Fig. 3. Experiments involved populations of 21 (*a*), 16 (*b*), 28 (*c*), and 6 (*d*) cells.

and more stable, reaching a statistically highly significant plateau ($p < 0.001$ for the difference between 30 data points acquired before and 4 min after increasing the glucose concentration to 30 mM). Thus, in one islet preparation in which five cells were analyzed simultaneously, the maximum luminescence increase, observed approximately 200 s after stimulation, was between 3.5 and 23.5% (Fig. 8*a*), indicative of β-cell heterogeneity (21).

Exposure to high external K^+ increased $[ATP]_c$ in β-cells highly reproducibly (Fig. 8*b*; Table I). Furthermore, simultane-

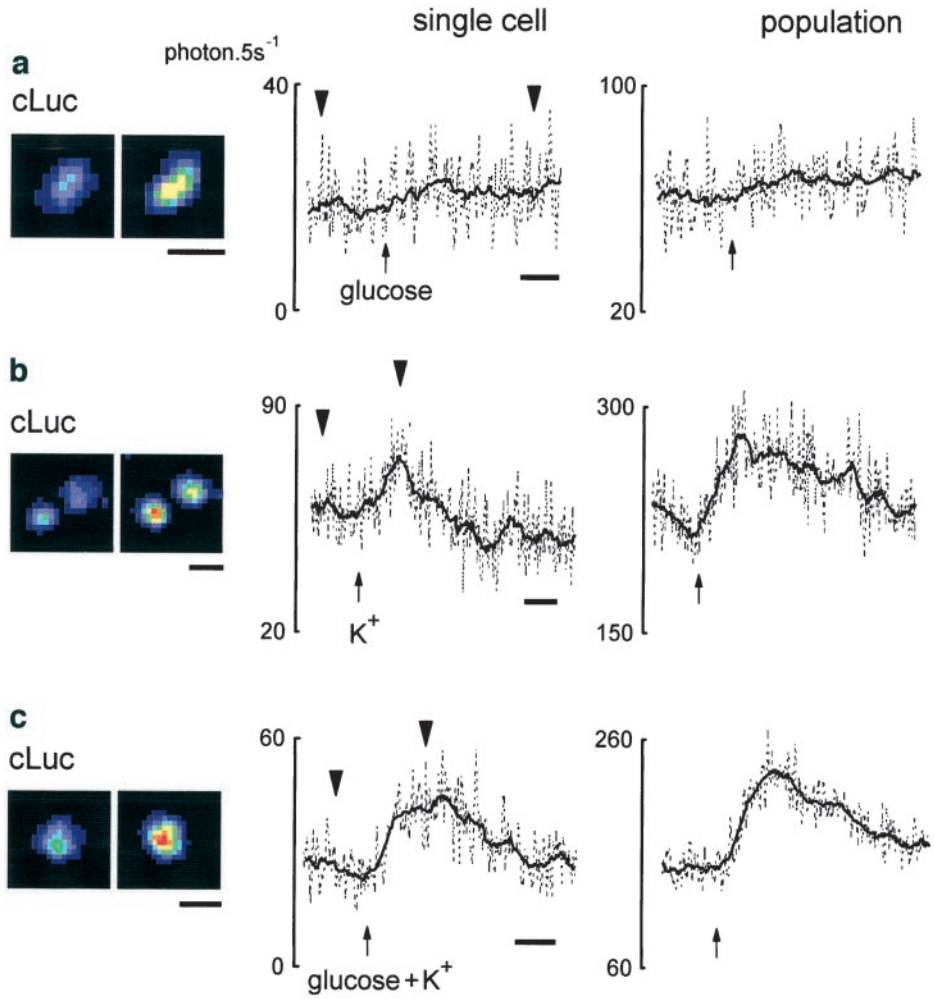

FIG. 8. **Glucose- and K^+-induced changes in $[ATP]_c$ in primary living β-cells.** Single primary β-cells or cell populations of 5–14 single β-cells were injected with plasmid cLuc and incubated for 10 min in 3 mM glucose before stimulation with 30 mM glucose (*a*), 70 mM K^+ (*b*), of 30 mM glucose plus 70 mM K^+ (*c*) (*upward arrows*). Photon counting imaging was performed as described under "Materials and Methods," and the *scale bars* and pseudocoloring are as in Fig. 3. Images of single cells (*a-c, insets*) correspond to photon production during 30-s integration beginning at the time points indicated by the *left* and *right downward arrows*.

ous addition of high glucose and high K^+ provided a luminescence increase that was larger and more rapid than the response to glucose alone (Fig. 8; Table I).

DISCUSSION

We describe here, for the first time, rapid dynamic imaging of free intracellular ATP concentration in subcompartments of single living cells. We show this to be feasible because the measured K_m values for ATP of each of the expressed recombinant luciferases were similar and in the low mM range. These values are much higher than those reported for purified firefly luciferase (*e.g.* 63 μM) (37, 51) and although we have not analyzed in detail the reason(s) for this, altered posttranslational modification of the enzyme seems possible. However, it might also be noted that our assay conditions, unlike those of the early *in vitro* studies, were designed to mimic the intracellular ionic environment and involved appropriate pH values, the presence of CoA, physiological salt concentrations, and high (1 mM) luciferin concentrations. However, our values are still lower than those obtained recently by Maechler *et al.* (19) who used an *in vivo* calibration approach. This involved the exposure of *Staphylococcus* α-toxin-permeabilized INS-1 cells to consecutive increases in [ATP]. However, permeabilization approaches are fraught with difficulties arising from the gradual leakage of luciferase, which can occur at very different rates for different individual cells. These authors (19), who made no adjustment for intracellular $[Mg^{2+}]$ or [CoA], obtained an apparent K_m for ATP of luciferase in excess of 10 mM. Whether our own values with extracted luciferase or those of Maechler *et al.* (19) provide the closest estimate of the true *in vivo* K_m of luciferase for ATP must be a matter of conjecture. Consequently, caution needs to be exercised when using *in vitro* determined K_m values for precise estimates of intracellular [ATP].

Resting [ATP] in β-Cell Subcompartments—Our data suggest that the concentration of [ATP] (predominantly as MgATP) is similar in three discrete domains of living islet β-cells, prior to elevations in extracellular glucose concentration, at around 1.0 mM. These values for cytosolic [ATP], which are lower than those of around 8 mM obtained by Maechler *et al.* (19), highlight a number of important features of β-cell metabolism and glucose sensing. First, given the electrogenic nature of the mitochondrial adenine nucleotide translocase (10), the similarity of $[ATP]_m$ and $[ATP]_c$ suggests that the free ADP concentration of mitochondria is likely to be considerably higher than in the bulk cytosol. Second, the data presented do not support the prediction that $[ATP]_{pm}$ may be substantially lower than $[ATP]_c$ in the resting β-cell, despite the requirement for active ion pumping, as demonstrated by the apparent increase in $[ATP]_{pm}$ in response to ouabain. This finding is congruent with data recently obtained by electrophysiological approaches in *Xenopus* oocytes (52). It therefore follows that inhibition of the K_{ATP} channel by ATP must involve changes in the concentration of this nucleotide in the mM range. Because the sensitivity of this channel to ATP is in the low μM range in inside-out patches (3), this might imply either that its ATP sensitivity is dramatically altered *in vivo* or that other factors lead to a decrease in its open-state probability at high glucose concentrations. Very recent data (53, 54) suggest that phos-

phatidyl inositol-4,5-bisphosphate is a likely candidate molecule.

Regulation of Mitochondrial ATP Synthesis by Glucose and Ca^{2+} Ions—In this work, we investigated first the regulation by glucose of $[ATP]_m$, because in this cell type, mitochondrial metabolism is likely to contribute to > 90% of all ATP synthesis (44, 55). Because resting $[ATP]_m$ was close to the observed K_m for ATP of firefly luciferase, glucose-induced increases in luminescence reported somewhat larger increases in $[ATP]_m$ (*e.g.* a 15% increase in luminescence would correspond to a 35% increase in $[ATP]_m$). We considered first how provision of the substrate, glucose, interacted with increases in intramitochondrial $[Ca^{2+}]$, to enhance respiratory chain activity and hence ATP synthesis. This is a complex problem because, according to the accepted view of metabolism-secretion coupling in the β-cell, some enhancement of ATP synthesis must occur in order to close K_{ATP} channels and hence increase $[Ca^{2+}]_c$ and $[Ca^{2+}]_m$. This should then enhance NADH production by mitochondrial dehydrogenases and hence substrate supply to the respiratory chain (12, 13, 56) and possibly the glycerol phosphate shuttle (55, 57–60). Furthermore, increases in $[Ca^{2+}]_m$ may enhance respiratory chain capacity directly (61, 62). Consistent with this model, increases in $[Ca^{2+}]_c$ have previously been shown to provoke elevations in the NAD(P)H/NAD^+ couple in β-cells (63)[2] and other cell types (64, 65). Our observations suggest that an increase in $[Ca^{2+}]_m$ in response to elevated glucose further enhances the increase in mitochondrial proton motive force provoked by elevated substrate supply alone. Indeed, when $[Ca^{2+}]_m$ was increased with no change in extracellular glucose (stimulation with K^+ the presence of extracellular Ca^{2+}, Fig. 5) we observed a parallel increase in both ΔΨ, and $[ATP]_m$. These data imply a permissive role for Ca^{2+} ions in glucose-induced free [ATP] increases. Lending further support to this view, high $[K^+]$ accelerated but did not substantially affect the maximum amplitude of glucose-induced increases in $[ATP]_c$ and $[ATP]_m$ in MIN6 cells, whereas it both accelerated and amplified the $[ATP]_{pm}$ change (Table I). Similarly, in primary β-cells, simultaneous addition of K^+ substantially increased the magnitude of the $[ATP]_c$ response to high glucose (Table I). However, in MIN6 cells, longer incubations (>400 s) with K^+ plus glucose led to a small decrease in $[ATP]_{pm}$ compared with values in the presence of glucose alone (results not shown), consistent with accelerated Ca^{2+} pumping in the sub-plasma membrane region and a gradual decline in mitochondrial proton motive force.

In apparent contrast to the present measurements of free [ATP] in discrete subcellular domains, it has been reported that in the intact islet, increases in total ATP content provoked by glucose were potentiated by pharmacological blockade of Ca^{2+} influx (14, 66, 67). However, careful inspection of other studies (68) suggests that elevation of intracellular $[Ca^{2+}]$ by K^+ plus diazoxide has no effect on, or causes a small increase in, total islet ATP content at high glucose concentrations. The differences between these earlier studies and the present work are likely to have several causes. First, it should be stressed that there is no *a priori* reason why total islet ATP content should directly represent free [ATP] in subdomains of the living β-cell, given the significant compartmentalization of ATP (for example, within an inert secretory granule pool) (69, 70), and the cellular heterogeneity of the islet (21). Second, when monitored dynamically in the present study, the effects of elevated K^+ on the response to glucose of [ATP] in each compartment were distinct and, in the case of $[ATP]_{pm}$, time-dependent. Finally, exocytosis from intact islets (or upstream steps such as vesicle mobilization) (71) may be more vigorous than in either isolated β-cells or the transformed MIN6 cell line. This would provide a greater ATP drain relative to ATP synthesis.

In the absence of external Ca^{2+}, K^+ stimulation resulted in a parallel decrease in ΔΨ, and $[ATP]_m$, as well as $[ATP]_{pm}$, presumably due to increased consumption of ATP by plasma membrane Na^+/K^+ and other ATPases. It follows, therefore, that the increases in $[ATP]_m$ prompted by K^+ in the presence of external Ca^{2+} are smaller than the overall increase in the rate of ATP synthesis, due to enhanced ATP consumption. However, an important exception to the close correlation between $[ATP]_m$ and ΔΨ, occurs during glucose stimulation in the presence of external Ca^{2+}. Here, increases in ΔΨ lag behind those of $[ATP]_m$ (Fig. 4). One possible explanation is that in these circumstances, a gradually increasing rate of increasing ATP synthesis is matched by increasing ATP consumption.

Regulation of $[ATP]_c$—In the β-cell, $[ATP]_c$ changes are likely to occur secondarily to $[ATP]_m$ increases. Intriguingly, the responses to extracellular glucose of $[ATP]_c$ and $[ATP]_m$ were found to differ in two important respects. First, elevated glucose provoked only a transient increase in $[ATP]_c$ compared the sustained increase seen in $[ATP]_m$. Second, $[ATP]_c$ but not $[ATP]_m$ increases were dependent upon increases in $[Ca^{2+}]_c$. These observations suggest that activation of mitochondrial ATP/ADP exchange may require elevations in intra- or extramitochondrial $[Ca^{2+}]$. It might be noted in this context that Ca^{2+} may increase dramatically the activity of the ADP/ATP translocase (72), a phenomenon possibly involved in the creation of nonspecific pores in the mitochondrial membrane during hypoxia and other cellular stresses (the "mitochondrial permeability transition") (73). The current data suggest that changes in intramitochondrial or cytosolic $[Ca^{2+}]$ might also have a role in the regulation of ATP/ADP translocase activity under nonpathological conditions. However, this would only be apparent when cytosolic $[Ca^{2+}]$ is increased, consistent with the fact that removal of extracellular Ca^{2+}, which is likely to cause a small decrease in resting intracellular $[Ca^{2+}]$, was without effect on $[ATP]_c$ or $[ATP]_m$.

Regulation of $[ATP]_{pm}$—In contrast to $[ATP]_c$, $[ATP]_{pm}$ remained elevated for up to 10 min after the beginning of incubation with 30 mM glucose. Thus, glucose appears to provoke the formation of a microdomain of [ATP] beneath the plasma membrane, which is regulated differently from [ATP] in the rest of the cytosol. How might this be achieved? As well as the activation of metabolism, increases in $[Ca^{2+}]_c$ are likely in the β-cell to profoundly increase ATP usage for processes such as secretory granule mobilization (71), exocytosis (74), extrusion of Ca^{2+} across the plasma membrane (75) and into intracellular stores (76), and activation of gene expression (77). Here, we provide evidence that during these events there may be preferential delivery of mitochondrial ATP to the sub-plasma membrane domain. Thus, the time course of changes in $[ATP]_{pm}$ following increases in extracellular glucose matched closely those of $[ATP]_m$. One explanation of the sustained elevation of $[ATP]_{pm}$ may therefore be that mitochondria at the cell periphery are exposed to more sustained $[Ca^{2+}]_m$ increases, as a result of glucose-activated Ca^{2+} influx, than those deeper within the cell. This would tend to prolong the activation of ATP synthesis in peripherally located mitochondria. Consistent with this, the return of $[ATP]_c$ to basal levels after K^+ stimulation was more rapid than that of $[ATP]_m$ or $[ATP]_{pm}$. Therefore, mitochondria located beneath the plasma membrane may provide a privileged domain of cytosolic [ATP], confined to this region of the cell. Such a role for strategically arranged mitochondria may also provide an explanation for the activation of exocytosis by the addition of certain mitochondrial

[2] E. K. Ainscow and G. A. Rutter, unpublished results.

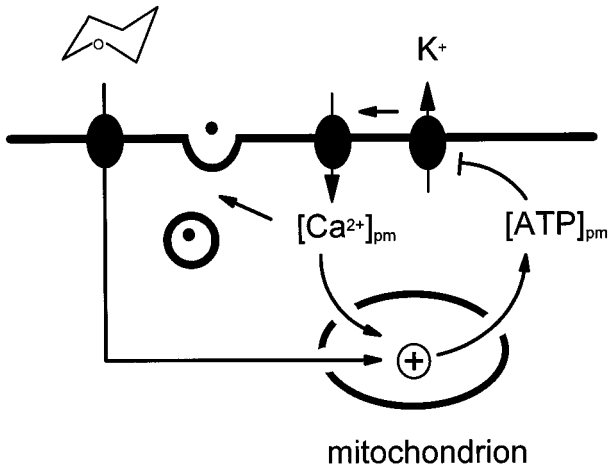

FIG. 9. **Scheme illustrating how peripherally localized mitochondria may participate in a glucose-activated feed-forward loop, generating locally high concentrations of ATP and Ca^{2+} beneath the plasma membrane, thus prompting exocytosis.**

substrates to permeabilized cells, despite the presence of high added MgATP concentrations (78). Alternatively, it is also conceivable that there are differences in the time course for the activation of ATP-consuming events at the plasma membrane (fusion of secretory vesicles or ion pumping), compared with those within the cytosol. Intriguingly, control of $[ATP]_{pm}$ in the β-cell would appear to be distinct from that in heart cells, where ATP derived from glycolysis appears preferentially to inhibit K_{ATP} channels (79, 80). On the other hand, recent data (81) suggest that mitochondria may play an important part in generating ATP microdomains close to the endoplasmic reticulum Ca^{2+}-ATPase of BHK-21 cells.

Oscillations in Intracellular [ATP] and Activated Insulin Secretion—Oscillatory release of insulin (82) may be essential to ensure normal glycaemia *in vivo* (83), although the mechanism(s) by which β-cells release insulin in an oscillatory fashion is not well understood (7). We occasionally observed oscillations in $[ATP]_{pm}$, although such oscillations were rare (data not shown). An important question is therefore whether oscillations in $[ATP]_{pm}$ and $[Ca^{2+}]_{pm}$ are causally linked.

Conclusion—We describe a new method for monitoring free ATP concentrations dynamically and in subdomains of single living cells. This technology should be applicable to the investigation of a wide variety of cell biological phenomena involving changes in intracellular [ATP] (84). With regard to the β-cell, perhaps the simplest model to explain our own observations is that an initial, small (Ca^{2+}-independent) increase in $[ATP]_m$, and subsequently in $[ATP]_{pm}$, may begin to close K_{ATP} channels, causing Ca^{2+} influx. This may then begin a "feed-forward" process, involving the further activation by Ca^{2+} of mitochondrial ATP synthesis and hence further closure of K_{ATP} channels (Fig. 9).

Acknowledgments—We thank Prof. J. I. Miyazaki for the provision of MIN6 β-cells. We also thank the Medical Research Council for providing an Infrastructure Award to establish the Bristol School of Medical Sciences Cell Imaging Facility, Profs. R. M. Denton and A. P. Halestrap for useful discussion, and Sara Ellis and Eleanor Basham for technical assistance.

REFERENCES

1. Ashcroft, F. M., and Kakei, M. (1989) *J. Physiol.* **416,** 349–367
2. Prentki, M., Tornheim, K., and Corkey, B. E. (1997) *Diabetologia* **40,** S32–S41
3. Ashcroft, F. M., Harrison, D. E., and Ashcroft, S. JH. (1984) *Nature* **312,** 446–448
4. Cook, D. L., and Hales, C. N. (1984) *Nature* **311,** 271–273
5. Rorsman, P. (1997) *Diabetologia* **40,** 487–495
6. Meglasson, M. D., Nelson, J., Nelson, D., and Erecinska, M. (1989) *Metabolism* **38,** 1188–1195
7. Civelek, V. N., Deeney, J. T., Kubik, K., Schultz, V., Tornheim, K., and Corkey, B. E. (1996) *Biochem. J.* **315,** 1015–1019
8. Detimary, P., Jonas, J. C., and Henquin, J. C. (1995) *J. Clin. Invest.* **96,** 1738–1745
9. Scholz, T. D., Laughlin, M. R., Balaban, R. S., Kupriyanov, V. V., and Heineman, F. W. (1995) *Am. J. Physiol.* **268,** H82–H91
10. Klingenberg, M. (1979) *Trends Biochem. Sci.* **4,** 249–252
11. Rothman, J. E. (1994) *Nature* **372,** 55–63
12. Denton, R. M., and McCormack, J. G. (1980) *FEBS Lett.* **119,** 1–8
13. McCormack, J. G., Halestrap, A. P., and Denton, R. M. (1990) *Physiol. Rev.* **70,** 391–425
14. Detimary, P., Gilon, P., and Henquin, J.-C. (1998) *Biochem. J.* **333,** 269–274
15. Rutter, G. A., White, M. R. H., and Tavare, J. M. (1995) *Curr. Biol.* **5,** 890–899
16. Kennedy, H. J., Viollet, B., Rafiq, I., Kahn, A., and Rutter, G. A. (1997) *J. Biol. Chem* **272,** 20636–20640
17. Bowers, K. C., Allshire, A. P., and Cobbold, P. H. (1992) *J. Mol. Cell Cardiol.* **24,** 213–218
18. Koop, A., and Cobbold, P. H. (1993) *Biochem. J.* **295,** 165–170
19. Maechler, P., Wang, H., and Wollheim, C. B. (1998) *FEBS Lett.* **422,** 328–332
20. Maechler, P., Kennedy, E. D., Wang, H., and Wollheim, C. B. (1998) *J. Biol. Chem.* **273,** 20770–20778
21. Pipeleers, D., Kiekens, R., Ling, Z., Wilikens, A., and Schuit, F. (1994) *Diabetologia* **37,** S57–S64
22. Bastianutto, C., Clementi, E., Codazzi, F., Podini, P., De Giorgi, F., Rizzuto, R., Meldolesi, J., and Pozzan, T. (1995) *J. Cell Biol.* **130,** 847–855
23. Rizzuto, R., Nakase, H., Darras, B., Francke, U., Fabrizi, G. M., Mengel, T., Walsh, F., Kadenbach, B., DiMauro, S., and Schon, E. A. (1989) *J. Biol. Chem.* **264,** 10595–10600
24. Rutter, G. A., Burnett, P., Rizzuto, R., Brini, M., Murgia, M., Pozzan, T., Tavare, J. M., and Denton, R. M. (1996) *Proc. Natl. Acad. Sci. U. S. A.* **93,** 5489–5494
25. Pouli, A. E., Karagenc, N., Bright, N., Arden, S., Schofield, G. S., Wasmeier, C., Hutton, J. C., and Rutter, G. A. (1998) *Biochem. J.* **330,** 1399–1404
26. Zhao, C., and Rutter, G. A. (1998) *FEBS Lett.* **430,** 213–216
27. Rizzuto, R., Simpson, A. W. M., Brini, M., and Pozzan, T. (1992) *Nature* **358,** 325–327
28. Woodward, R. H. (1972) in *Statistical Methods in Research and Production* (Davies, O. L., and Goldsmith, P. L., eds) pp. 178–236, Longman Group Ltd., London
29. Stanley, P. E., and Williams, S. G. (1969) *Anal. Biochem.* **29,** 381–392
30. Pfanner, N., and Meijer, M. (1997) *Curr. Biol.* **7,** R100–R103
31. Hess, D. T., Slater, T. M., Wilson, M. C., and Skene, J. H. (1992) *J. Neurosci.* **12,** 4634–4641
32. Rizzuto, R., Brini, M., Pizzo, P., Murgia, M., and Pozzan, T. (1995) *Curr. Biol.* **5,** 635–642
33. Marsault, R., Murgia, M., Pozzan, T., and Rizzuto, R. (1997) *EMBO J.* **16,** 1575–1581
34. Tagaya, M., Genma, T., Yamamoto, A., Kozaki, S., and Mizushima, S. (1996) *FEBS Lett.* **394,** 83–86
35. Liang, Y., and Matschinsky, F. M. (1991) *Diabetes* **40,** 327–333
36. Ford, S. R., Buck, L. M., and Leach, F. R. (1995) *Biochim. Biophys. Acta* **1252,** 180–184
37. DeLuca, M., Wannlund, J., and McElroy, W. D. (1979) *Anal. Biochem.* **95,** 194–198
38. Sherf, B. A., and Wood, K. V. (1994) *Promega Notes* **49,** 14–21
39. Kennedy, H. J., Viollet, B., Kahn, A., and Rutter, G. A. (1997) *Diabetic Med.* **14** S8
40. Craig, F. F., Simmonds, A. C., Watmore, D., McCapra, F., and White, M. R. H. (1991) *Biochem. J.* **276,** 637–641
41. Corkey, B. E., Duszynski, J., Rich, T. L., Matschinsky, B., and Williamson, J. R. (1986) *J. Biol. Chem.* **261,** 2567–2574
42. Rutter, G. A., Osbaldeston, N. J., McCormack, J. G., and Denton, R. M. (1990) *Biochem. J.* **271,** 627–634
43. Wang, X., Levi, A. J., and Halestrap, A. P. (1996) *Am. J. Physiol* **270,** H476–H484
44. Panten, U., and Klein, H. (1982) *Endocrinology* **111,** 1595–1600
45. Robb-Gaspers, L. D., Burnett, P., Rutter, G. A., Denton, R. M., Rizzuto, R., and Thomas, A. P. (1998) *EMBO J.* **17,** 4987–5000
46. Nicholls, D. G. (1982) *Bioenergetics: An Introduction to the Chemiosmotic Theory*, Academic Press, London
47. Rutter, G. A. (1999) in *Imaging Living Cells* (Rizzuto, R., and Fasolato, C., eds) pp. 286–300, Springer-Verlag, Heidelberg
48. Cobbold, P. H., and Lee, J. A. C. (1991) in *Cellular Calcium: A Practical Approach* (McCormack, J. G., and Cobbold, P. H., eds) pp. 55–81, Oxford University Press, Oxford, United Kingdom
49. Nakazaki, M., Ishihara, H., Kakei, M., Inukai, K., Asano, T., Miyazaki, J. I., Tanaka, H., Kikuchi, M., Yada, T., and Oka, Y. (1998) *Diabetologia* **41,** 279–286
50. Pipeleers, D. G. (1992) *Diabetes* **41,** 777–781
51. Lemasters, J. J., and Hackenbrock, C. R. (1977) *Biochemistry* **16,** 445–447
52. Gribble, F. M., Tucker, S. J., and Ashcroft, F. M. (1998) *Diabetologia* **41,** A13
53. Shyng, S. L., and Nichols, C. G. (1998) *Science* **282,** 1138–1141
54. Baukrowitz, T., Schulte, U., Oliver, D., Herlitze, S., Krauter, T., Tucker, S. J., Ruppersberg, J. P., and Fakler, B. (1998) *Science* **282,** 1141–1144
55. Sekine, N., Cirulli, V., Regazzi, R., Brown, L. J., Gine, E., Tamarit-Rodriguez, J., Girotti, M., Marie, S., MacDonald, M. J., Wollheim, C. B., and Rutter, G. A. (1994) *J. Biol. Chem.* **269,** 4895–4902
56. Rutter, G. A. (1990) *Int. J. Biochem.* **22,** 1081–1088
57. MacDonald, M. J. (1981) *J. Biol. Chem.* **256,** 8287–8290
58. Meglasson, M. D., Smith, K. M., Nelson, D., and Erikinsca, M. (1989) *Am. J. Physiol.* **19,** E173–E178
59. Sener, A., and Malaisse, W. J. (1992) *J. Biol. Chem.* **267,** 13251–13256
60. Rutter, G. A., Pralong, W.-F., and Wollheim, C. B. (1992) *Biochim. Biophys.*

Acta **1175,** 107–113
61. Halestrap, A. P. (1982) *Biochem. J.* **204,** 37–47
62. Robb-Gaspers, L. D., Rutter, G. A., Burnett, P., Hajnoczky, G., Denton, R. M., and Thomas, A. P. (1998) *Biochim. Biophys. Acta.* **1366,** 17–32
63. Pralong, W. F., Bartley, C., and Wollheim, C. B. (1990) *EMBO J.* **9,** 53–60
64. Rizzuto, R., Bastianutto, C., Brini, M., Murgia, M., and Pozzan, T. (1994) *J. Cell Biol.* **126,** 1183–1194
65. Hajnoczky, G., Robb-Gaspers, L. D., Seitz, M. B., and Thomas, A. P. (1995) *Cell* **82,** 415–424
66. Ohta, M., Nelson, J., Nelson, D., Meglasson, M. D., and Erecinska, M. (1993) *J. Pharmacol. Exp. Ther.* **264,** 35–40
67. Panten, U., and Lenzen, S. (1988) in *Energetics of Secretion Responses* (Akkerman, J. W. N., ed) pp. 109–123, CRC Press, Boca Ranton, FL
68. Detimary, P., Van den Berghe, G., and Henquin, J.-C. (1996) *J. Biol. Chem.* **271,** 20559–20565
69. Hutton, J. C., Penn, E. J., and Peshavaria, M. (1983) *Biochem. J.* **210,** 297–305
70. Detimary, P., Jonas, J. C., and Henquin, J. C. (1996) *Endocrinology* **137,** 4671–4676
71. Pouli, A. E., Emmanouilidou, E., Zhao, C., Wasmeier, C., Hutton, J. C., and Rutter, G. A. (1998) *Biochem. J.* **333,** 193–199
72. Brustovetsky, N., and Klingenberg, M. (1996) *Biochemistry* **35,** 8483–8488
73. Halestrap, A. P., Griffiths, E. J., and Connern, C. P. (1993) *Biochem. Soc. Trans.* **21,** 353–358
74. Weber, T., Zemelman, B. V., McNew, J. A., Westermann, B., Gmachl, M., Parlati, F., Sollner, T. H., and Rothman, J. E. (1998) *Cell* **92,** 759–772
75. Carafoli, E. (1987) *Annu. Rev. Biochem.* **56,** 395–433
76. Rutter, G. A., Theler, J.-M., Li, G., and Wollheim, C. B. (1994) *Cell Calcium* **16,** 71–80
77. Rafiq, I., Kennedy, H. J., and Rutter, G. A. (1998) *J. Biol. Chem.* **273,** 23241–23247
78. Maechler, P., Kennedy, E. D., Pozzan, T., and Wollheim, C. B. (1997) *EMBO J.* **16,** 3833–3841
79. Weiss, J. N., and Lamp, S. T. (1987) *Science* **238,** 67–69
80. Weiss, J., and Hiltbrand, B. (1985) *J. Clin. Invest.* **75,** 436–447
81. Landolfi, B., Curci, S., Debellis, L., Pozzan, T., and Hofer, A. M. (1998) *J. Cell Biol.* **142,** 1235–1243
82. Lang, D. A., Matthews, D. R., Burnett, M., and Turner, R. C. (1981) *Diabetes* **30,** 435–439
83. O'Rahilly, S., Turner, R. C., and Matthews, D. R. (1988) *N. Engl. J. Med.* **318,** 1225–1230
84. Szewczyk, A., and Pikula, S. (1998) *Biochim. Biophys. Acta* **1365,** 333–353
85. Rutter, G. A., and Denton, R. M. (1988) *Biochem. J.* **252,** 181–189

Glucose Generates Sub-plasma Membrane ATP Microdomains in Single Islet β -Cells: POTENTIAL ROLE FOR STRATEGICALLY LOCATED MITOCHONDRIA

Helen J. Kennedy, Aristea E. Pouli, Edward K. Ainscow, Laurence S. Jouaville, Rosario Rizzuto and Guy A. Rutter

J. Biol. Chem. 1999, 274:13281-13291.
doi: 10.1074/jbc.274.19.13281
